

## 69. OPAQUE MINERALOGY OF BASEMENT ROCKS, LEG 37

James M. Hall, Department of Geology, Dalhousie University,  
Halifax, Nova Scotia, Canada

and

Joseph F. Fischer, Department of Geology, The University of Texas at Arlington,  
Arlington, Texas

### INTRODUCTION

Opaque minerals are minor phases in all the basement rocks recovered during DSDP Leg 37. However, they are of greater interest and importance than their relatively small presences might suggest. Thus the titanomagnetites, the most susceptible minerals to oxidation, can contribute significantly to our knowledge of the progress of the alteration of upper Layer 2 as the plate travels away from the median valley of the Mid-Atlantic Ridge. Again, the state of the titanomagnetite controls the magnetic state of the basement rocks, of which the basalts in particular must generate at least the major part of the linear magnetic anomaly patterns found over the ocean basins. The spinels, which are of the chromium-magnesium-aluminum type, always occur as phenocrysts. This type of occurrence contrasts strongly with that of the titanomagnetite. Mantling and reaction rims tell us about the change in physical and chemical conditions between the magma at depth and during eruption.

The sulfides are important in that they tell us, when primary, about oxygen and sulfur fugacity during initial crystallization and cooling, and when secondary, about hydrothermal or halmyrolitic alteration. We should also keep in mind that sulfides are important ore minerals, but their iron-rich compositions, and low abundances in the Leg 37 basement holes, do not encourage us to think of oceanic Layer 2 from this part of the world as a future source of ores.

### GENERAL REMARKS ON THE OCCURRENCE AND DISTRIBUTION OF OPAQUE PHASES

Most microscope work was carried out using a Zeiss Ultraphot at a magnification of 625 diameters.

The opaque minerals are here taken to include the titanomagnetites, sulfides, and spinels, although the latter are not strictly opaque. In general there is about 1% by volume of these minerals in the basalts, of which most is titanomagnetite. Sulfides occupy rather less than 1% of the samples, and often less than 0.01%, but only a few samples appear entirely free of a primary sulfide phase. Spinel is relatively rare.

Titanomagnetite occurs strictly as a microlitic phase. Phenocrysts were not found, and therefore are presumed not to be a factor in differentiation of the lavas. The microlites are generally in the 1  $\mu\text{m}$ -50  $\mu\text{m}$  size range, occurring with glass, smectites altered from glass, or in variolitic clusters of plagioclase and pyroxene.

Primary sulfides occur commonly in globular form and are restricted to the mesostasis. The globular morphology is highly suggestive of immiscible liquid origin. Very few of samples lack sulfide globules, although amounts and sizes are always relatively small.

Secondary sulfides, almost entirely pyrite, are most abundant in veins and altered zones near veins within the basalts, and are most prominent in the massive basalts.

Chromium-magnesium-aluminum spinel occurs sporadically, restricted to relatively primitive magmas. About 5% of the rocks studied contain this mineral.

### OXIDES IN BASALTS

There are two oxide minerals in the basalts, titanomagnetite, with its partly oxidized counterparts, and (CrMgAl) spinel. Titanomagnetite is by far the most abundant, occurring ubiquitously, while spinel is restricted both in number of occurrences and in abundance where it does occur.

#### Titanomagnetite

The chemistry and structure of the titanomagnetites present vary widely. We can show from rock magnetic and ore microscope studies that the compositional variation in the titanomagnetite immediately following initial cooling of the basalts was in contrast, very limited, and that the present variation is the result of oxidative halmyrolitic alteration of the basalts. Curie point measurements, combined with the degree of reversibility of curves of the temperature dependence of saturation magnetization (Hall and Ryall, this volume) together with ore microscope observations, indicate that initially titanomagnetites with  $x$  in  $x\text{Fe}_2\text{TiO}_4 \cdot (1-x)\text{Fe}_3\text{O}_4$  at  $0.64 \pm 0.02$  characterized the basalts. Only one sample (332B-8-1, 106-108 cm, Plate 3, Figure 1) in the set of 425 basalts studied contains titanomagnetite that presently has the stoichiometric composition given above. With a few exceptions, all the others contain cation deficient titanomagnetite, or titanomaghemite, with a wide range in degree of cation deficiency. From the rock magnetic measurements, we find that the peak in the distribution of cation deficiency for the basalt titanomagnetites is for  $0.6 < z < 0.8$ , where  $z$  is the fraction of  $\text{Fe}^{2+}$  oxidized to  $\text{Fe}^{3+}$  in the oxide. The cation deficiency that occurs during this oxidation process is the result of the need to maintain overall electro-neutrality in the lattice while the average positive charge of the iron ions increases.

The recognition of the presence of cation-deficient titanomagnetite in these basalts by the conventional ore microscope method is frequently prevented by the small size of the grains, with consequent difficulty in identifying colors or internal features of the grains. Hence our dependence on rock magnetic properties for this information. The characteristic small size of individual titanomagnetite grains is the result of the rapid quenching of the basalts in the subaqueous environment. This leads to an abundance of individual incomplete crystals and crystallites (Plate 1, Figures 1-3; Plate 2, Figure 5; Plate 4, Figures 3, 4). Characteristic grain dimensions of less than 5  $\mu\text{m}$  are widespread and very few samples have grains with dimensions in excess of 20  $\mu\text{m}$ . Crystal form is typically skeletal, with a trend to anhedral form (Plate 1, Figure 4) in the few relatively coarse grained samples.

Deuteric oxidation, characterized by ilmenite exsolution lamellae in magnetite, which is widespread in subaerial basalts, is present in at the most three samples: 332B-33-2, 85-88 cm (1); 332B-44-5, 61-63 cm (1); and 333A-6-2, 92-94 cm (2). Even here the evidence is largely from magnetic properties; all three samples are fine grained with tiny gray to silvery oxides set in red or orange stained silicates.

Since cation deficiency is so widespread in the titanomagnetites, and is of such significance in determining the magnetic properties of the basalts, we have given considerable attention to visible evidence for its presence (Plate 3, Figures 1-4, Plate 4, Figures 1-4).

Two distinct types of alteration features, volume change cracks and lightening in color, characterize the cation-deficient titanomagnetites. The features are sometimes clearly sequential, with lightening following cracking and sometimes independent, as when lightening occurs apparently without previous cracking. Volume change cracking, which we suppose is associated with chemical changes occurring during oxidation, is evident at even very low levels of cation deficiency. Thus, the typical curved cracks are seen in Plate 3, Figures 3 and 4 where  $z$  is 0.44 and 0.35, respectively, while by the time  $z$  reaches 0.45 (Plate 4, Figure 1) the cracks are very widely developed. In contrast, color lightening, which is most easily seen when contrasts occur within one grain or between adjacent grains, is not evident until  $z \cong 0.50$ . In many cases (Plate 4, Figures 3 and 4), areas of different colors within one grain are clearly bounded by volume change cracks, so confirming the sequence of alteration indicators. However, in some samples, illustrated by Plate 4, Figure 5, color lightening is clearly peripherally distributed. The apparent absence here of a phase of volume change cracking is not understood. With the onset of color lightening at  $z \cong 0.50$ , evidence of the alteration of the titanomagnetites is also seen in the adjacent silicates. We see a dull orange-brown staining of silicates adjacent to the oxides, and of the rock as a whole, at the highest  $z$  levels. This effect is readily interpreted in terms of the expulsion of iron from the oxides, so forming the lattice vacancies responsible for their cation deficiency. This is an important result since it bears on the process of the formation of cation-

deficient oxides. Clearly, this occurs by iron expulsion rather than oxygen accretion.

### Chrome-Magnesium-Aluminum Spinel

Spinel is an uncommon phase found in only a few of the rocks. Basalt 335-5-3, 55-57 cm is an exception; here spinel amounts to 5% of the rock. The spinels are generally in the size range 10  $\mu\text{m}$ -100  $\mu\text{m}$ , relatively euhedral, and are translucent reddish-brown in color when seen in thin section.

The spinels are most abundant as inclusions in olivine phenocrysts, and less abundant in the groundmass, usually close to olivines. They are generally fresh; a few, however, have incipient reaction margins to magnetite (Plate 6, Figures 2-5). These margins preserve the former spinel shapes, and are clearly a reaction between the crystal and liquid, and not an overgrowth. Vermiform patterns with glass patches in these zones suggest net loss of crystalline material.

Chemical analysis (Sigurdsson; Flower et al., this volume) suggests that the spinels have  $\text{Cr}/(\text{Cr} + \text{Al})$  of 0.4-0.6 and  $\text{Mg}/(\text{Mg} + \text{Fe}'')$  of 0.6-0.75 and are not markedly different from other Mid-Atlantic Ridge spinels.

The spinels from the highly phyrlic basalts near the bottom of Hole 332A are much larger than the average. The phenocrysts (or possibly xenocrysts) are up to 2 mm in diameter and are the typical reddish-brown translucent color. These grains have abundant large fluid or gas inclusions.

### Ilmenite

We searched for primary ilmenite in association with titanomagnetite, in the hope that oxygen fugacities during crystallization might be obtained from microprobe analysis of the coexisting phases (Buddington and Lindsley, 1964). However, ilmenite was never certainly identified, extending our evidence for stating that the mineral is very much rarer in oceanic submarine basalts than it is in subaerial basalts.

## HYDROXIDES

We described above how, when titanomagnetite was in a high state of cation deficiency, the surrounding silicates were stained in brown or orange tints. It seems reasonable to assume that the coloration is the result of the presence of finely disseminated iron hydroxides. Massive secondary hydroxides are found as veins and patches in the more altered basalts (Plate 5, Figures 1-5). No analyses have been made of these phases as yet, although their frequent relatively large size makes them suitable for microprobe investigations.

## OXIDES IN PLUTONIC ROCKS

### Chromium-Magnesium-Aluminum Spinel (Plate 6)

The spinel phase of the plutonic rocks consists of scattered anhedral chromite grains, both individually and within olivine crystals, and is of generally less than 1 mm in diameter. These spinels are brownish, translucent chromite, with both  $\text{Cr}/(\text{Cr} + \text{Al})$  and  $\text{Mg}/(\text{Mg} + \text{Fe})$  ratios very close to 0.5 (Clarke and Loubat;

Sigurdsson; Symes et al., all this volume). They plot in the overlap field of alpine and stratiform complexes.

### Secondary Magnetite

The serpentinized peridotites contain abundant fine magnetite resulting from olivine breakdown (Plate 7, Figures 1 and 2). Rock magnetism measurements indicate that the magnetite is indistinguishable from pure  $\text{Fe}_3\text{O}_4$ . The magnetite occurs as individual grains, clusters, and chains. Its presence accounts for the strong magnetization of these rocks and its occurrence in continuous chains across polished surfaces implies that high electrical conductivity should also be a characteristic.

## SULFIDES (PLATE 2)

### Sulfides in Basalts

Primary sulfide grains of very small size and frequently of globular form occur scattered throughout the glass phase of the basalts. Most of the primary sulfides are less than  $5\ \mu\text{m}$  in diameter, making optical study difficult. Microprobe analysis totals are consistently low due to fluorescence in the surrounding glass (MacLean, this volume). The globular morphology is indicative of an origin as an immiscible sulfide liquid in the silicate melt.

Optically, most of the grains less than  $5\ \mu\text{m}$  across appear to be homogeneous. Larger grains, however, show some anisotropy; in some globules there are at least two phases, both as apparent primary crystallization phases from the sulfide liquid and as definite exsolution lamellae.

The main phase is pyrrhotite; a less abundant primary phase appears to be chalcopyrite, and where exsolution occurs the lamellae also appear to consist of chalcopyrite. Bulk microprobe analyses (MacLean, this volume) show only a few percent of Cu and less than 1% of Ni in pyrrhotite globules.

The globules occur mainly in the residual glass phases. However, in some rocks there are globules within the variolitic radial sheaves of microlites and, rarely, within microlites. Samples without globules are rare. There appears to be no relationship between general grain size or position within a pillow and globule size or abundance.

The globules are closely spherical except where they have grown on preexisting titanomagnetite; here they tend to hemispherical. The globules contain phases other than sulfides, amounting to about 30% of the total volume. It is presumed that this is silicate glass (or crystals) which was miscible in the sulfide phase.

Naldrett et al. (this volume) measured average sulfur contents in the basalts at close to 250 ppm, and they suggest that this value is 25%-30% of the expected value for a basaltic magma which is saturated with sulfur. The late appearance of globules within the crystallizing basalt suggests that the basalts were indeed strongly undersaturated with respect to sulfur at the time of extrusion and that saturation was not reached until at least half of the liquid had crystallized. The Ni content of the basalts is normal; the low values of the Ni in the sulfides are probably due to previous partitioning into olivine.

### Secondary Sulfides in Basalts

There are pyrite-bearing joint surfaces scattered sporadically throughout the sampled sequences of basalt flows. These veins are more obvious in the massive microdiabasic rocks than in the pillowed flows, but are not restricted to them.

Pyrite crystals range up to  $1/2\ \text{mm}$  across and occur both on the vein surfaces and in alteration halos associated with these veins. Large crystals may be abundant in vesicles near the veins, or replace parts of the groundmass.

Pyrite is also present in the chinks and oozes interlayered with or overlying the basalt sequences. Determination of  $\text{S}^{34}$  values strongly suggests a certain amount of bacterial sulfate reduction. It also tends to indicate that secondary sulfides at shallow levels are more nearly in equilibrium with seawater than those deep in the pillow pile, which are closer to magmatic values. Thus there appears to be a regular trend with depth, implying that the pyrite formed after the entire sequence, and some of its sedimentary cover was emplaced.

The source of the sulfur for the pyrite does not appear to be the lavas themselves. However the isotopic relationships do not clearly distinguish between hydrothermal solutions from a deeper magmatic source or a seawater source. Although either is possible, a deep magmatic source with seawater contamination is favored by us, particularly in view of the relatively non-oxidative alteration associated with the pyrite.

In rare cases—e.g., plutonic Sample 334-20-2 (# 1A) and basaltic Sample 333A-6-1, 13-15 cm—there is clear-cut evidence that the secondary sulfides are later than the smectite alteration. In the first rock cited, pyrite occurs as botryoidal crusts on clay linings of veins, with further clay crystallization on the crusts. In a second rock—333A-6-1, 13-15 cm—there are several pyrrhotite (?) clumps with radial growth morphology of individual grains. One of these in particular has grown in a smectite pseudomorph after olivine.

## SULFIDES IN PLUTONIC ROCKS

The sulfide phases in the plutonic rocks are the most varied. In these rocks pyrite, pyrrhotite, chalcopyrite, pentlandite, and bornite were identified. For the most part, the sulfides occur in brecciated and serpentinized areas; they are absent from the fresh material. It then would appear that the minerals are mainly of a secondary origin, and may even have followed the emplacement of the plutonic rocks into the shallow crustal level at which they presently are found.

### ACKNOWLEDGMENTS

Sample preparation, examination, and photography were carried out by Tim Milligan and Jeff Clarke, to whom we offer our gratitude. Osama Abdel-Aal and Dan Plasse gave critical reviews of the first draft of the manuscript. Mary Ann Annand typed the manuscript.

### REFERENCE

- Buddington, A.F. and Lindsley, D.H., 1964. Iron-titanium oxide minerals and synthetic equivalents: *J. Petrol.*, v. 5, p. 310.

PLATE 1

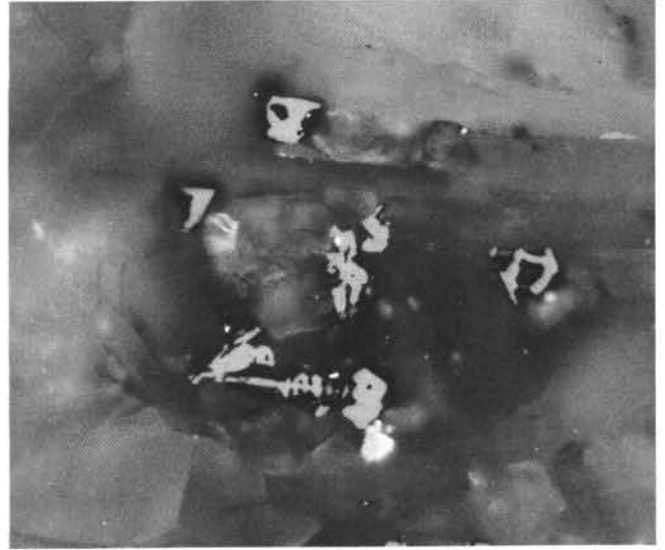
Typical forms for titanomagnetite. Scale bar is equal to 20  $\mu\text{m}$ .

- Figure 1      Fine-grained skeletal titanomagnetite (off white) and small rounded sulfides (white) (332B-35-3, 69-72 cm).
- Figure 2      Medium skeletal titanomagnetite (gray) and sulfide (white) (332A-12-1, 108-111 cm).
- Figure 3      Large skeletal titanomagnetite (333A-10-2, 112-115 cm).
- Figure 4      Anhedral titanomagnetite (332A-31-3, 70-73 cm [2]).

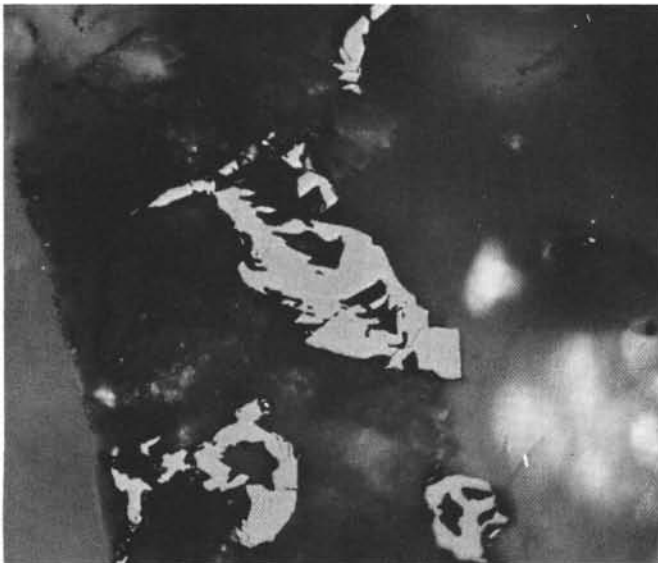
PLATE 1



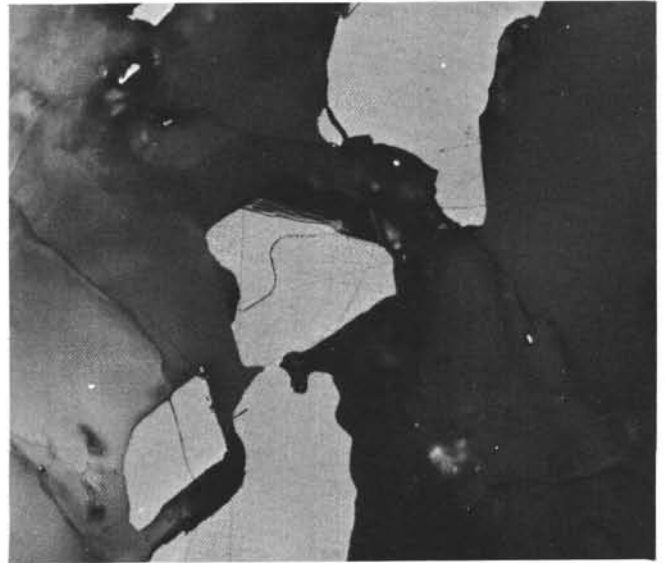
1



2



3



4

20μm

PLATE 2

Sulfides (note that primary sulfides are also seen in some photographs of oxides). Scale bar is equal to 20  $\mu\text{m}$ .

- Figure 1 Primary iron sulfide globule (332B-3-3, 119-122 cm).
- Figure 2 Anhedral primary iron sulfides (332A-33-2, 61-64 cm) [2].
- Figure 3 Primary iron sulfide (white) mantled with secondary magnetite (gray) derived from the serpentinization of olivine (334-22-4, 95-97 cm [2]).
- Figure 4 Primary iron sulfides, two phases, white and gray in angular enclosures, mantled by secondary magnetite (gray) (334-22-2, 61-63 cm [2]).
- Figure 5 Secondary pyrite (white, irregular form) with primary skeletal magnetite (335-13-2, 13-22 cm).
- Figure 6 Secondary pyrite veining in massive basalt (333A-10-1, 31-39 cm [2.1]).

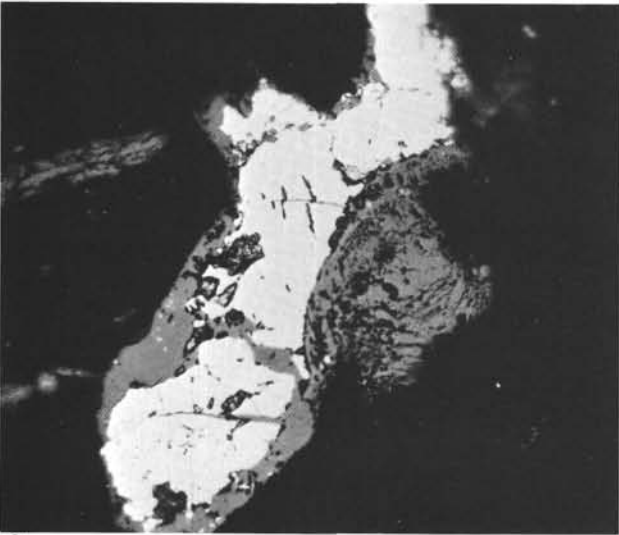
PLATE 2



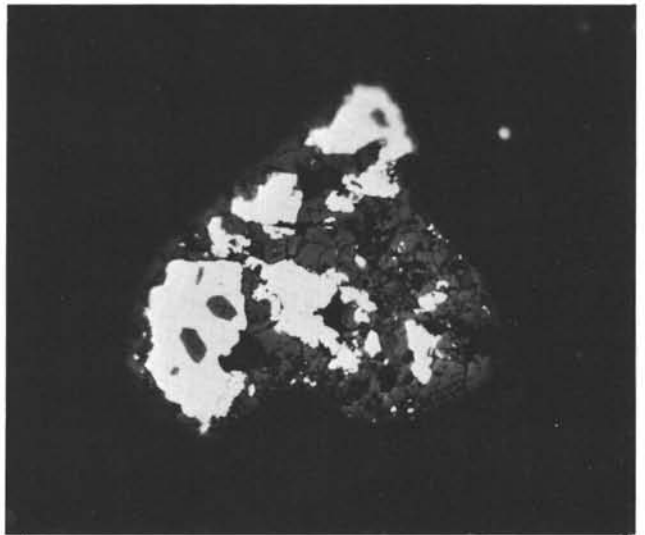
1



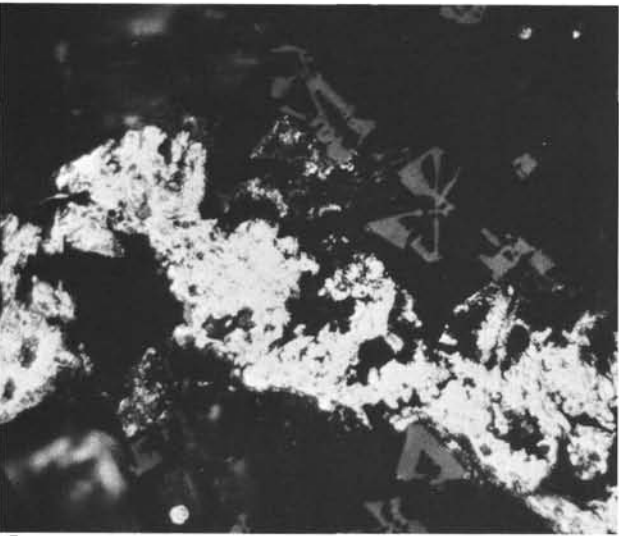
2



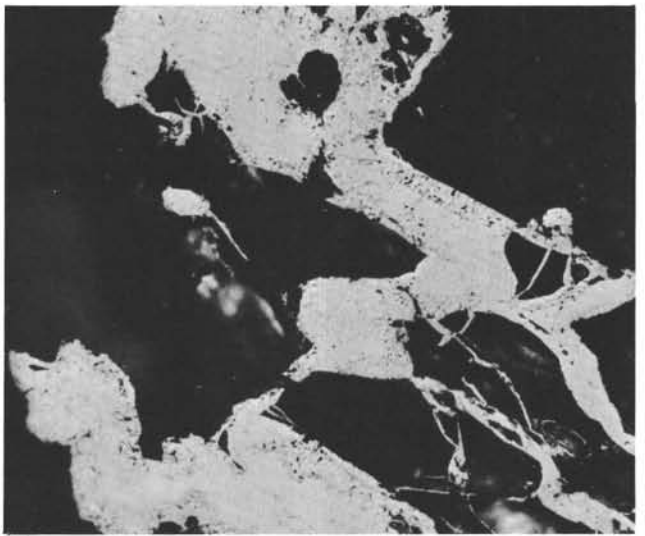
3



4



5



6

20µm

PLATE 3

Low temperature oxidation of titanomagnetite.  
Scale bar is equal to 20  $\mu\text{m}$ .

- Figure 1 Stoichiometric titanomagnetite (gray)—note the uniform color and lack of cracking—and iron sulfide (white) (332B-8-1, 106-108 cm).
- Figure 2 The first signs of volume change cracking in titanomagnetite (332B-96-2, 32-34 cm [2.1]).
- Figure 3 Minor volume change cracking in titanomagnetite (gray) and iron sulfide (white) (334-16-2, 109-112 cm)i
- Figure 4 Minor volume change cracking in titanomagnetite (light gray), small iron sulfides (white) (332A-31-3, 70-73 cm [2]).

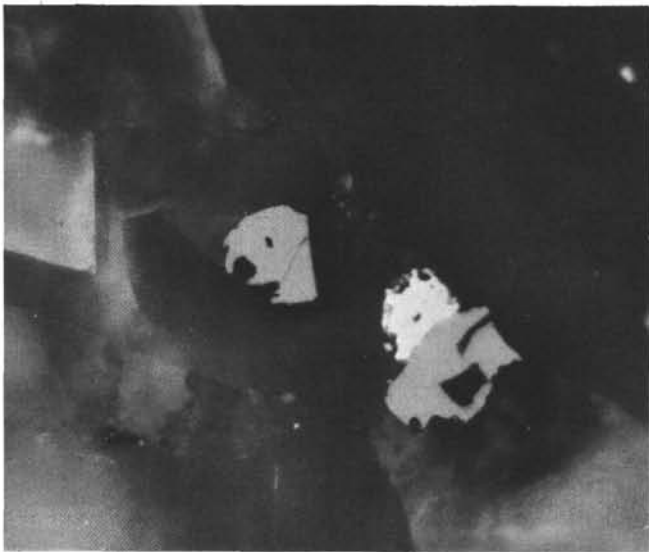
PLATE 3



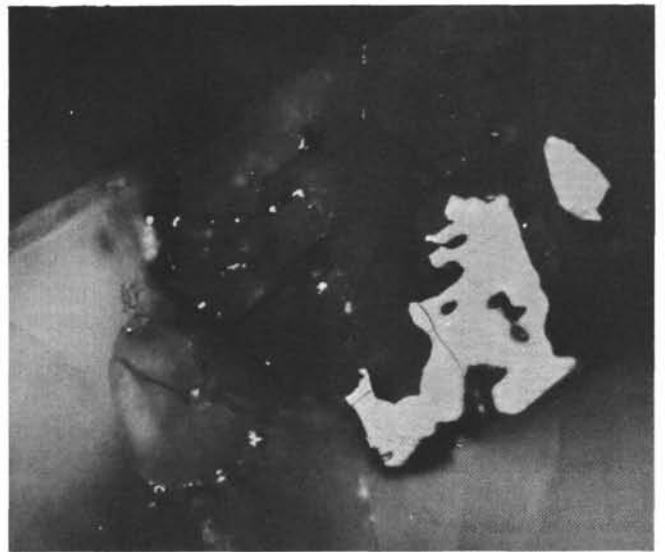
1



2



3



4

20  $\mu$ m

PLATE 4

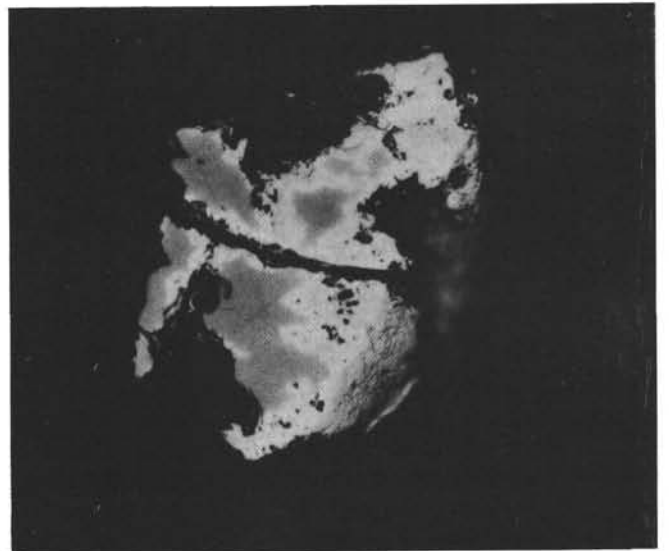
Low temperature oxidation of titanomagnetite.  
Scale bar is equal to 20  $\mu\text{m}$ .

- Figure 1 Strongly developed volume change cracking in titanomagnetite (334-16-2, 109-112 cm).
- Figure 2 Peripheral lightening of titanomagnetite (332B-9-2, 104-106 cm).
- Figure 3 Patchy whitening of titanomagnetite with the different areas bounded by volume change cracks (334-17-3, 3-6 cm [2]).
- Figure 4 Patchy whitening of titanomagnetite with the different areas bounded by volume change cracks (334-19-3, 93-95 cm).

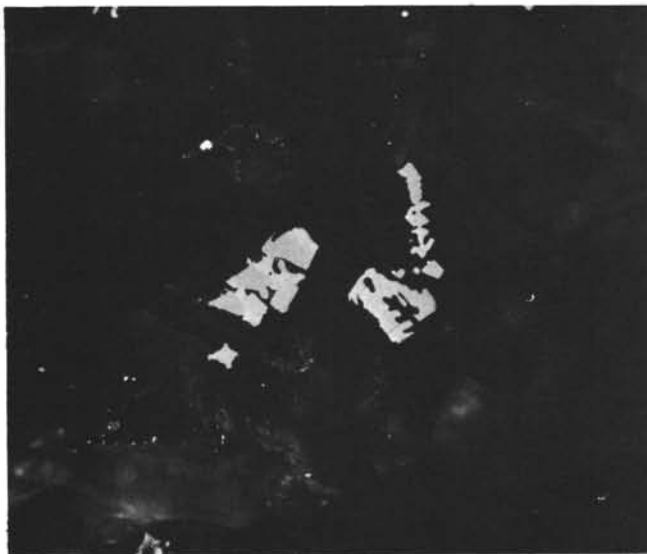
PLATE 4



1



2



3



4

20  $\mu$ m

PLATE 5

Secondary iron oxides and hydroxides.

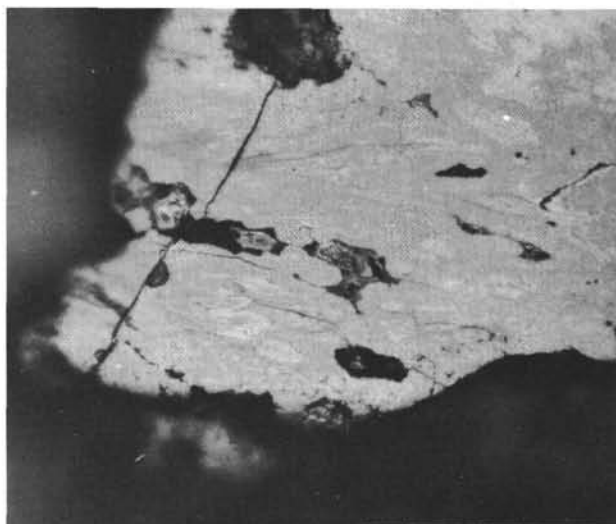
Scale bar is equal to 20  $\mu\text{m}$ .

- Figure 1      Massive iron hydroxide (332A-14-1, 93-96 cm [4]).
- Figure 2      Possible titanomagnetite xenocryst altered by  
reaction (332B-25-4, 47-49 cm).
- Figure 3      Massive iron hydroxide in vein strongly red  
stained from finely disseminated iron hydroxide  
(335-6-1, 53-55 cm).
- Figure 4      Primary skeletal titanomagnetite showing patchy  
whitening (top) adjacent to iron hydroxides  
masses (below) (332B-9-1, 112-113 cm).
- Figure 5      Massive iron hydroxide within veinfilling, stained  
red by finely disseminated hematite or iron  
hydroxide (332B-35-1, 33-36 cm [2]).

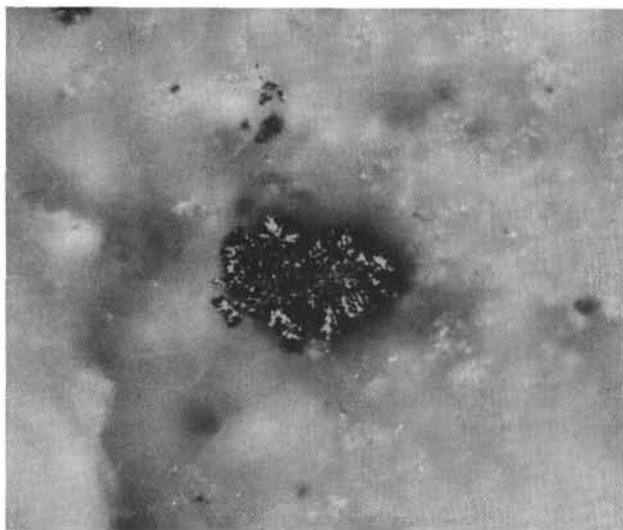
PLATE 5



1



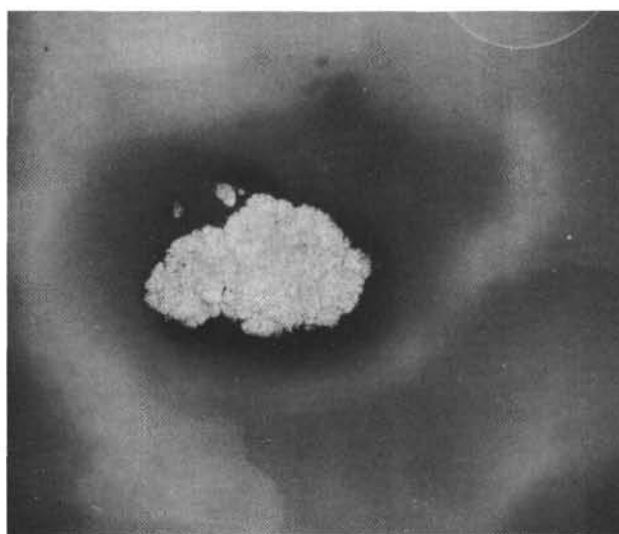
2



3



4



5

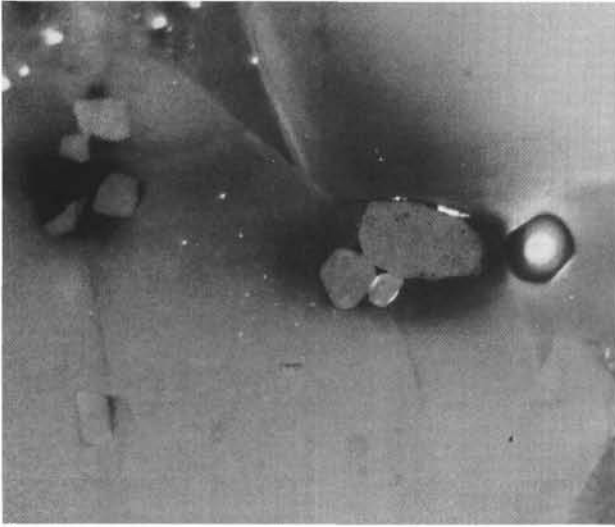
20μm

PLATE 6

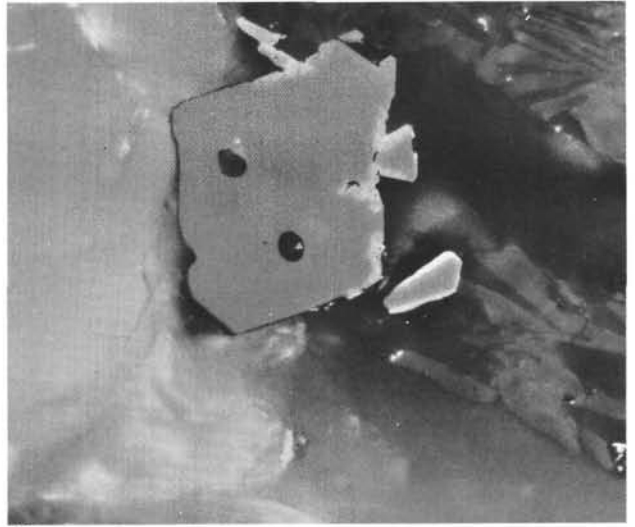
Spinels. Scale bar is equal to 20  $\mu\text{m}$ .

- Figure 1      Spinel (gray) (332B-19-1, 75-78 cm).
- Figure 2      Spinel showing peripheral alteration (332B-25-3, 28-31 cm [4]).
- Figure 3      Spinel showing reticulate peripheral alteration suggesting a reaction relationship (332B-35-3, 69-72 cm).
- Figure 4      The details of reticulate peripheral alteration in a spinel xenocryst (335-16-1, 22-24 cm [2.1]).
- Figure 5      Spinel rimmed with whitened titanomagnetite (lower) and a vesicle lined with iron hydroxide (upper) (332B-18-1, 43-45 cm).

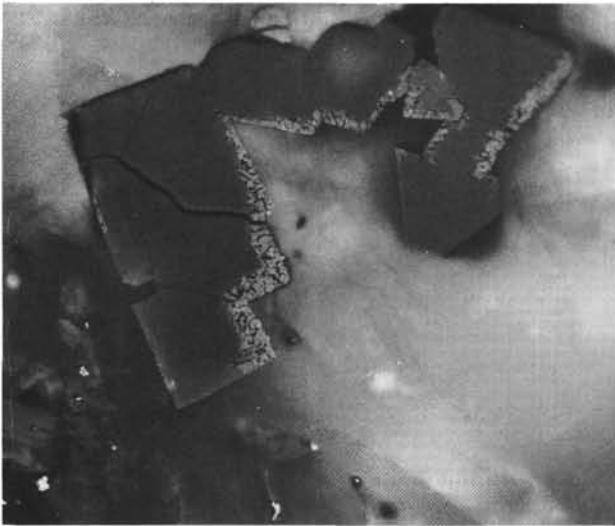
PLATE 6



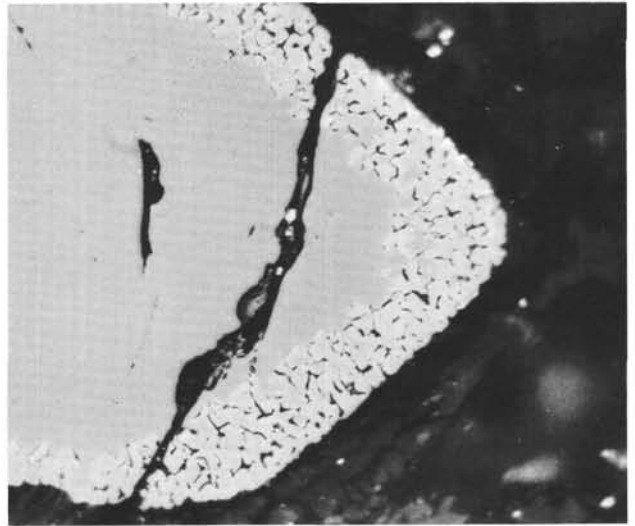
1



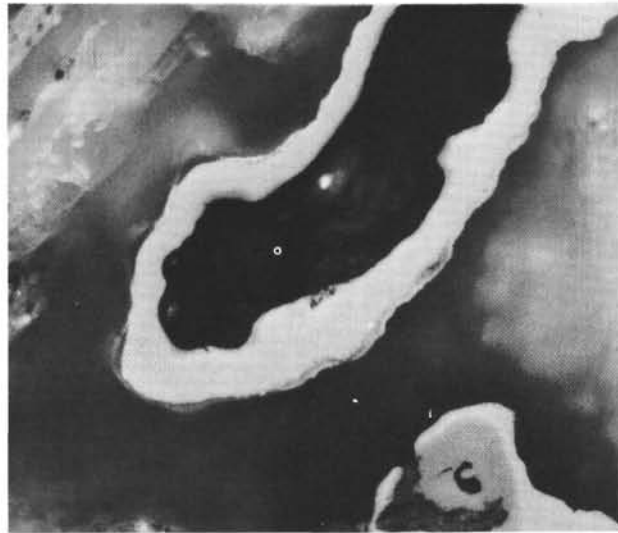
2



3



4



5

20µm

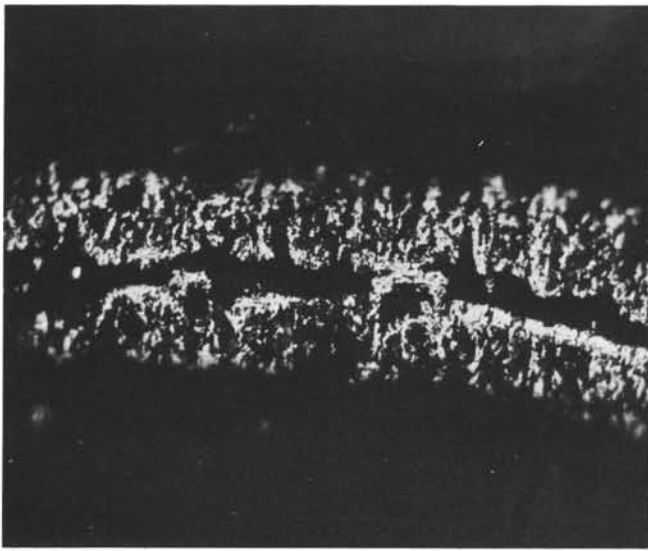
PLATE 7

Magnetite from the serpentinization of olivine.

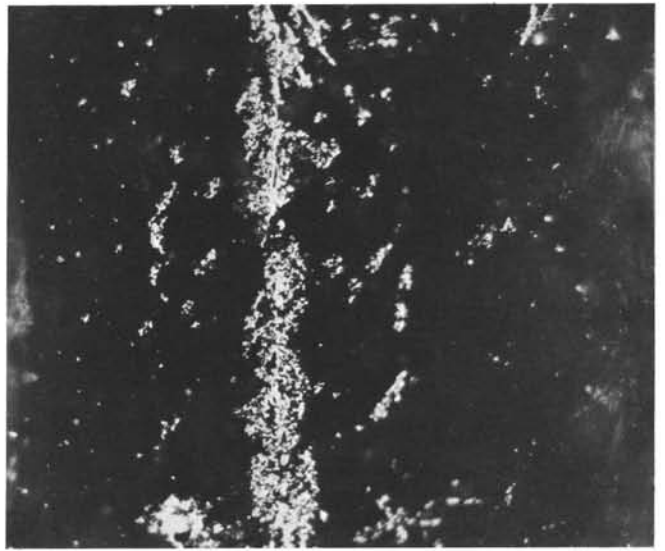
Scale bar is equal to 20  $\mu\text{m}$ .

- Figure 1 Chains and individual grains of magnetite after olivine (334-22-2, 61-63 cm).
- Figure 2 Chains, patches, and individual grains of magnetite after olivine (334-22-4, 95-97 cm [2]).

PLATE 7



1



2

20µm